Progress In Electromagnetics Research, Vol. 150, 41–48, 2015

Efficient Evaluation of Near-Field Time-Domain Physical-Optics Integral Using Locally Expanded Green Function Approximation

Xiao Zhou and Tie Jun Cui*

Abstract—A time-efficient method is proposed to calculate the near-field time-domain physical-optics (TD-PO) integral to analyze the transient electromagnetic fields scattered from three-dimensional perfectly conducting objects under the illumination of a pulsed plane wave. It is shown that the TD-PO integral can be reduced to a close-form expression by introducing locally expanded Green-function approximations used in conjunction with the surface partitioning. As a result, the near-field TD-PO response to a general pulsed plane wave excitation is derived by a convolution of the excitation waveform with the TD-PO impulse response, which can be performed in a closed form. To satisfy the causality, i.e., the transient field cannot travel away from the sources faster than the speed of light, the high-order derivative of a modulated-Gaussian wave is specified as the excitation waveform. The efficiency and accuracy of the proposed near-field formulas are validated through numerical examples.

1. INTRODUCTION

The interest in the analysis of transient wave phenomena has been growing primarily due to the many recent advances which are taking place in the development of ultra-wide band (or short pulse) radar and their associated antennas for remote sensing and target identification applications; in addition, there has always been significant interest in the effects of natural and man-made electromagnetic pulse (EMP) on complex radiating systems such as aircraft and spacecraft. It is natural to analyze transient electromagnetic (EM) wave phenomena directly in the time domain (TD). Even though conventional frequency-domain (FD) solution, in conjunction with fast Fourier transform (FFT) can be employed to obtain TD solutions, it is very time consuming since a wide frequency range needs to be considered. There are various numerical TD methods such as finite-difference time-domain (FDTD) or TD integral equation approaches, but these numerical solutions for analyzing transient phenomena become intractable when the pulse width of transient incident field is very narrow compared with the geometrical dimensions of scattering object. Recently, direct use of physical optics (PO) in the time domain has been of interest [1–3]. The advantages are several. These quasi-analytical solutions can provide closed form solutions which contain physical interpretation of transient wave behavior. Furthermore, they also provide efficient and faster computation, more suitable solutions when pulse width is narrow compared with the geometrical dimensions of scattering object, and feasibility to implement a hybrid solution by combination with various time domain methods such as FDTD [4, 5].

In the conventional physical optics (PO) method, the fields scattered by a metallic plate S of arbitrary shape have been given by a surface integral. The computation time to evaluate this surface integral by numerical integration increases rapidly with the increase of electrical size of scattering surfaces. Thus, the numerical evaluation of such a surface integral is time-consuming, which becomes the crux of PO technique. Recently, we have reduced this surface integral to a line integral for time-domain far-field calculations. When S is a polygon, the line integral is further reduced to a closed-form

Received 25 October 2014, Accepted 1 December 2014, Scheduled 21 December 2014
* Corresponding author: Tie Jun Cui (tjcui@seu.edu.cn).
The authors are with the State Key Laboratory of Millimeter Waves, Southeast University, Nanjing 210096, China.

expression [6], which is very similar to the well-known Gordon formula in the evaluation of PO integral in the frequency domain [7]. These closed-form far-field expressions are not dependent on the size of the scattering surface with respect to the wavelength (minimum wavelength of the spectrum for time-domain calculations) [6–8]. Only functional evaluations are required in these closed-form expressions without quadrature errors, and the evaluation perform more efficient than numerical quadrature techniques [8], such as Gauss-Legendre Quadrature (GLQ).

One such assumption for these closed-form PO representations, both in time domain and frequency domain, is that the observation point is located at infinity. The most obvious way to evaluate the PO integral in the near-field observation is to rely on quadrature techniques by employing an exact Green function. This provides excellent accuracy, but the computational burden will become significant for electric-large targets. Legault [9] provided an alternative approach relying on a phase approximation of the same order as the one used in the far-field close-form formulas. This approach requires very little increase in computational cost, yields excellent accuracy in the near field, and becomes practically attractive in the evaluation of the frequency-domain near-field PO integral. However, all the previous work on the reduction and evaluation of the near-field PO surface integrals has been considered in the frequency domain. The main point of the this paper is to provide an efficient evaluation of PO integral in time domain when the observer is in the near-field of the scatterer. As a nature extension of our previous work in evaluation of far-filed TD-PO integral [6], we propose a close-form near-field time-domain expression by introducing locally expanded Green function approximations which is considered by Legault [9] in frequency domain. To the authors' best knowledge, this is the first time that an efficient approach for evaluation of the near-field PO integral is provided in the time domain.

In this paper, the near-field TD-PO response to a general pulsed plane wave excitation is found by a convolution of the excitation waveform with the TD-PO impulse response. The near-field TD-PO impulse response performs in a closed form and behaves as a superposition of rectangular window functions. For solving a true time-domain problem in physics, one has to reply on the (mathematical) uniqueness of the associated initial-value problem. Thus, to satisfy causality (the transient field cannot travel away from the sources faster than the speed of light) [10], high-order derivative of modulated-Gaussian wave is specified as the excitation waveform.

The rest of the paper is organized as follows. The near-field TD-PO integral of interest is derived in Section 2. To this end, a perfect electrically conducting (PEC) object illuminated by a pulsed plane wave is considered. Then, by using locally expanded Green function approximations in time domain, a closed-form formula for the transient scattering electric field observed in the near field is derived. Numerical examples that prove the efficacy of using the proposed approach are presented in Section 3. Conclusions are stated in Section 4.

2. NEAR-FIELD TD-PO FORMULATIONS AND EQUATIONS

In this section, the derivation of the near-field TD-PO electromagnetic computing formulas is taken in TD directly. The proposed near-field expression will be used to analyze the transient scattering from large PEC objects illuminated by a pulsed plane wave. The incident time domain plane wave of the transient scattering problem is given by

$$\mathbf{E}^i\left(\mathbf{r}',t\right)=\hat{\mathbf{e}}^i E_{inc}\left(t-\hat{\mathbf{k}}^i\cdot\mathbf{r}'/c\right)\varepsilon\left(t-\hat{\mathbf{k}}^i\cdot\mathbf{r}'/c\right) \tag{1}$$

where $\hat{\mathbf{k}}^i$ is the normalized incident-wave vector, $\hat{\mathbf{e}}^i$ the normalized polarization direction of the incident wave, $E_{inc}(t)$ the time-domain incident electric field intensity, and $\varepsilon(t)$ the step function. Note that $\mathbf{E}^i(\mathbf{r}',t)\equiv 0$ for $t<\hat{\mathbf{k}}^i\cdot\mathbf{r}'/c$, and the time reference $t=0$ is selected at $\mathbf{r}'=(0,0,0)$, which allows $t<0$ for a negative value of $\hat{\mathbf{k}}^i\cdot\mathbf{r}'/c$.

2.1. Near-filed TD-PO Surface Integral

Given the geometry of the PEC targets and the transient incident field, beam tracing technique is then used to find the lit region described in terms of triangles. By using the vector-potential solution to

Maxwell's equations for E and H fields and the physical optics approximation, we assume

$$\mathbf{J}\left(\mathbf{r}',t\right)=2\hat{\mathbf{n}}\times\left[\frac{\hat{\mathbf{k}}^{i}\times\mathbf{E}^{i}\left(\mathbf{r}',t\right)}{\eta_{0}}\right]=\frac{\hat{\mathbf{j}}}{\eta_{0}}E_{inc}\left(t-\hat{\mathbf{k}}^{i}\cdot\mathbf{r}'\right)\varepsilon\left(t-\hat{\mathbf{k}}^{i}\cdot\mathbf{r}'/c\right) \tag{2}$$

where $\mathbf{J}\left(\mathbf{r}',t\right)$ denotes the current density in the PO lit region, $\hat{\mathbf{j}}=2\hat{\mathbf{n}}\times\hat{\mathbf{k}}^{i}\times\hat{\mathbf{e}}^{i}$, $\hat{\mathbf{n}}$ the outward normal unit vector to the lit surface, and η_0 intrinsic impedance of free space. The near-field expression of the time-domain PO integral can be given as [11]

$$\begin{aligned}\mathbf{E}^{s}\left(\mathbf{r},t\right)=&-\frac{1}{4\pi}\int_{S}\left[\frac{\hat{\mathbf{j}}-\hat{\mathbf{R}}\left(\hat{\mathbf{R}}\cdot\hat{\mathbf{j}}\right)}{cR}\frac{\partial}{\partial t}E_{inc}\left(t-\hat{\mathbf{k}}_{i}\cdot\mathbf{r}'/c-R/c\right)+\frac{\hat{\mathbf{j}}-3\hat{\mathbf{R}}\left(\hat{\mathbf{R}}\cdot\hat{\mathbf{j}}\right)}{R^{2}}E_{inc}\left(t-\hat{\mathbf{k}}_{i}\cdot\mathbf{r}'/c-R/c\right)\right.\\&\left.+\frac{\hat{\mathbf{j}}-3\hat{\mathbf{R}}\left(\hat{\mathbf{R}}\cdot\hat{\mathbf{j}}\right)}{R^{3}/c}\int_{t_{0}}^{t-\hat{\mathbf{k}}_{i}\cdot\mathbf{r}'/c-R/c}E_{inc}\left(t'\right)dt'\right]dS'\end{aligned} \tag{3}$$

2.2. Reduction of the Surface Integral to a Closed-form Formula

Following the procedure of frequency-domain near-filed method developed in [9], we write

$$R=\frac{\mathbf{r}-\mathbf{r}_{n}{}'}{\left|\mathbf{r}-\mathbf{r}_{n}{}'\right|}\cdot\left(\mathbf{r}-\mathbf{r}'\right)=\hat{\mathbf{k}}_{n}\cdot\left(\mathbf{r}-\mathbf{r}'\right) \tag{4}$$

where $\mathbf{r}_{n}{}'$ is an arbitrary expansion center, which is always chosen at the center of a polygonal element. Applying this locally expanded approximation of R, time-domain Green function is approximated as

$$\frac{1}{R}\delta\left(t-R/c\right)\approx\frac{1}{R_{n}}\delta\left[t-\frac{\hat{\mathbf{k}}_{n}\cdot\left(\mathbf{r}-\mathbf{r}'\right)}{c}\right] \tag{5}$$

with the same amplitude and a linear time decay variation on the surface. When S is a metallic plate of N-polygonal shape, the scattering field in (3) can be simplified as

$$\mathbf{E}^{s}\left(\mathbf{r},t\right)=-\frac{1}{4\pi}\left[\frac{\hat{\mathbf{j}}-\hat{\mathbf{R}}_{n}\left(\hat{\mathbf{R}}_{n}\cdot\hat{\mathbf{j}}\right)}{cR_{n}}E_{inc}\left(t\right)+\frac{\hat{\mathbf{j}}-3\hat{\mathbf{R}}_{n}\left(\hat{\mathbf{R}}_{n}\cdot\hat{\mathbf{j}}\right)}{R_{n}^{2}}E_{inc}^{-1}\left(t\right)+\frac{\hat{\mathbf{j}}-3\hat{\boldsymbol{R}}_{n}\left(\hat{\mathbf{R}}_{n}\cdot\hat{\mathbf{j}}\right)}{R_{n}^{3}/c}E_{inc}^{-2}\left(t\right)\right]*W\left(t\right) \tag{6}$$

where

$$W\left(t\right)=\int_{S}\frac{\partial}{\partial t}\delta\left(t-\hat{\mathbf{k}}_{i}\cdot\mathbf{r}'/c-\hat{\mathbf{k}}_{n}\cdot\left(\mathbf{r}-\mathbf{r}'\right)/c\right)dS' \tag{7}$$

$$\begin{aligned}E_{inc}^{-1}\left(t\right)&=\int_{t_{0}}^{t}E_{inc}\left(t'\right)dt'\\E_{inc}^{-2}\left(t\right)&=\int_{t_{0}}^{t}E_{inc}{}^{-1}\left(t'\right)dt'\end{aligned} \tag{8}$$

Note that the convolution $E_{inc}^{(m)}(t-\tau)=E_{inc}^{(m)}(t)*\delta(t-\tau)$ has been used to obtain (6). As a natural application of our previous work in [6], $W(t)$ in (7) can be written as the following closed-form representation:

$$W\left(t\right)=\begin{cases}\delta'\left(t-\tau_{\mu}\right), & \left|\boldsymbol{\alpha}\right|=0\\\displaystyle\sum_{\mu=1}^{3}I_{\mu}\left(t\right), & \left|\boldsymbol{\alpha}\right|\neq0\end{cases} \tag{9}$$

$I_\mu(t)$ is the contribution of the μth side of S to $W(t)$ and may be written as

$$I_{\mu}\left(t\right)=\frac{c}{\left|\boldsymbol{\alpha}\right|^{2}}\begin{cases}\boldsymbol{\alpha}^{*}\cdot\Delta\mathbf{v}_{\mu}\delta\left(t-\tau_{\mu}\right), & \boldsymbol{\kappa}\cdot\Delta\mathbf{v}_{\mu}=0\\\boldsymbol{\alpha}^{*}\cdot\Delta\mathbf{v}_{\mu}\left[\varepsilon\left(t-\tau_{\mu}\right)-\varepsilon\left(t-\tau_{\mu+1}\right)\right]/\boldsymbol{\kappa}\cdot\Delta\mathbf{v}_{\mu}, & \boldsymbol{\kappa}\cdot\Delta\mathbf{v}_{\mu}\neq0\end{cases} \tag{10}$$

In the above equation, $\boldsymbol{\alpha}$ is the projection of the vector $\boldsymbol{\kappa} = \hat{\mathbf{k}}^i - \hat{\mathbf{k}}_n$ on the polygonal surface; $\boldsymbol{\alpha}^*$ is a vector obtained by rotating $\boldsymbol{\alpha}$ through an angle of 90°; $\mathbf{v}_1$, $\mathbf{v}_2$, ..., $\mathbf{v}_N$ are the position vectors of the vertices of a polygonal surface in the global coordinate; for $1 \leq \mu \leq N$, $\Delta\mathbf{v}_\mu = \mathbf{v}_{\mu+1} - \mathbf{v}_\mu$, $\mathbf{v}_N = \mathbf{v}_1$; $\varepsilon(t)$ is the step function; $\delta'(t)$ is the derivative of the delta function $\delta(t)$. The time decay is related to each vertice of the polygon which is given by

$$\tau_\mu = t_d + (r + \boldsymbol{\kappa} \cdot \mathbf{v}_\mu)/c \tag{11}$$

Note that $|\boldsymbol{\alpha}|$ in (9) and $\boldsymbol{\kappa} \cdot \Delta\mathbf{v}_\mu$ in (10) may not be equal to zero for the most observation directions, and thus $W(t)$ will be written as a superposition of rectangular window functions. For the relevant proofs to hold, the exciting sources always have to start at some instant time in the finite past of the observation and cease at instant another time. Assume that the electric and magnetic fields satisfy causality, the sources are located in a bounded volume, and the sources are zero everywhere for $t < t_0$. Then the scattering field $\mathbf{E}^s(\mathbf{r}, t)$ in (3) and (6) are zero everywhere for $t < t_0$ and $t \to \infty$. As a result, the excitation waveform in (6) must satisfy the follow condition:

$$\begin{aligned} &E_{inc}^{(-2)}(t) \equiv 0, \quad t < t_0 \\ &\int_{t_0}^{t} E_{inc}^{(-2)}(\varsigma)\, d\varsigma = 0, \quad t \to \infty \end{aligned} \tag{12}$$

In this paper, the high-order (≥ 2) derivative of modulated-Gaussian-impulse plane wave is used because it includes a finite band of time as well as a finite band of frequency, and it has no zero points in their spectrum. Third-order derivative of modulated-Gaussian-impulse is used in Section 3 because it allows that the time-domain convolution in (6) can be taken only by functional evaluations without numerical quadrature.

3. NUMERICAL EXAMPLES AND DISCUSSIONS

In this section, numerical examples that demonstrate the accuracy of the derived formula and the efficiency achieved are given. The transient results of the derived near-field closed-form expression (nfTDPO), as well as the incident waveform, have been transformed to the frequency domain, and the normalized results (nfTDPO-FFT) are then compared to the normalized results obtained from the near-field formula proposed by Legault in [9] in frequency-domain (nfFDPO) and the results obtained by using four-point Gauss-Legendre Quadrature (GLQ4) evaluation. It is worth noting that the amplitudes of the incident electric field for nfFDPO and GLQ4 calculations are fixed to be 1 V/m for all frequencies. We also give the comparison of computation time to demonstrate and discuss the advantage of using the proposed near-field closed-form representation for the TD-PO integrals over the numerical (GLQ) evaluation. All scatterers are illuminated by the same pulsed plane wave. The incidence electric field is expressed in (1), and the temporal behavior of the incidence plane wave is given by a third-order derivative of the modulated-Gaussian pulse (see Fig. 1(a)), which is defined by

$$E_{inc}(t) = A(t) \exp\left(-\frac{4\pi(t-t_0)^2}{\tau^2}\right) \tag{13}$$

where $\omega = 2\pi f_0$, and $f_0 = 10\,\text{GHz}$, $\tau = 1.0\,\text{ns}$, $t_0 = 0.8\,\text{ns}$ for the following examples, and $A(t)$ is the modulated amplitude for TD electric field which is given as

$$\begin{aligned} A(t) = \frac{1}{\tau^6}\Big[&-8\pi(t-t_0)\left(8\pi\left(8\pi(t-t_0)^2 - 3\tau^2\right) - 3\omega^2\tau^4\right)\cos(\omega t) \\ &+\omega\tau^4\left(24\pi\left(-8\pi(t-t_0)^2 + \tau^2\right) + \omega^2\tau^4\right)\sin(\omega t)\Big] \end{aligned} \tag{14}$$

The maximum value of $E_{inc}(t)$ is just the the maximum amplitude of $A(t)$.

The first example is a PEC rectangular plate. The plate lies on the x-y plane with edge length $a = 0.6\,\text{m}$. The incident angle of the pulsed plane wave is 0 degrees off the normal, and the observation point is at (0, 0, 0.50 m) (see Fig. 1(b)). The PO lit region is trivially formulated as a union of two triangular surfaces. In order to compute the transient scattering field using nfTDPO and nfFDPO

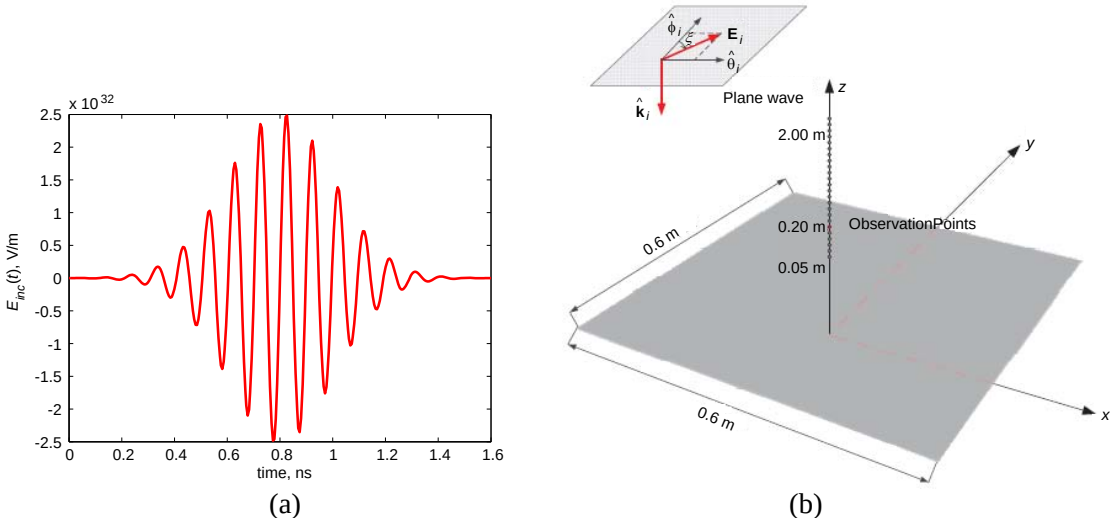

Figure 1. (a) The waveform of the incident plane wave. (b) Canonical problem of near-field transient scattering from a rectangular plate. Observation at $z = 0.05 \sim 2.00$ m, $x = y = 0$ m.

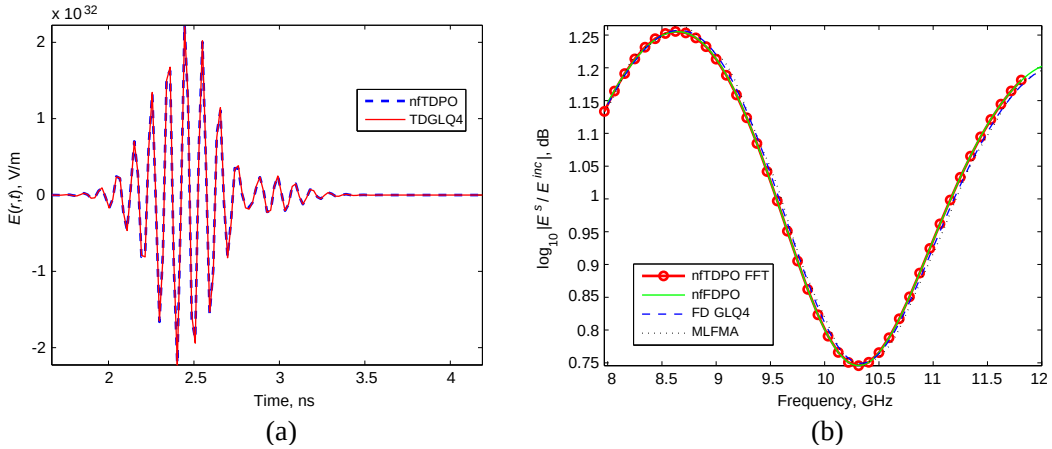

Figure 2. (a) The near-field transient response of backscattering from a rectangular plate at $z = 0.50$ m, $x = y = 0$ m (refers to Fig. 1). (b) The normalized wideband near-field frequency-domain results of backscattering from the rectangular plate.

Table 1. Path number and computation times.

	Path Number: $\sum_{i=1}^{N_{Obs}} N_i/N_{Obs}$			Computation Times [s]		
Examples	nfTDPO	nfFDPO	TD-GLQ4	nfTDPO	nfFDPO	TD-GLQ4
1	481	481	147968	0.083	0.076	29.554
2	396	396	147968	26.410	6.867	13938 (3.87 h)
3	36689	36689	-	89.256	240.013	-

solutions, those two triangular surfaces has to be subdivided into 481 sub-triangles ($D_n < \sqrt{R\lambda_{\min}/2}$) in order to properly evaluate the time-domain or frequency-domain PO integrals. In the GLQ4 solution, they have been modelled by 147968 sub-triangles (see Table 1) whose edge lengths measure less than $\lambda_{\min}/10$ to achieve excellent accuracy. The transient electric-field results obtained by nfTDPO and

time-domain GLQ4 (TD-GLQ4) are plotted in Fig. 2(a), and the wideband nfTDPO-FFT results are plotted in Fig. 2(b). The FD results are then compared to the frequency-domain ones obtained from the nfFDPO, frequency-domain GLQ4 (FD-GLQ4), as well as the result based on multilevel fast multipole algorithm (MLFMA). As can be seen, the agreement is perfect. The path number and computation times of nfTDPO, nfFDPO and TD-GLQ4 are compared in Table 1. It is interesting to note that the ratio of the computation time of the proposed method (nfTDPO) to TD-GLQ4 method is about 1 : 3561. The speed of the computation time of nfFDPO is better than nfTDPO because only a few sampled frequencies (101) are needed for these smooth results.

As the second example, the transient results scattering from the PEC rectangular plate at different observation points are investigated. The observation points are located at z-axis with the range from $z = 0.05\,\text{m}$ to $2.00\,\text{m}$. The transient electric-field results obtained by nfTDPO solutions are plotted in Fig. 3(a) ($\log_{10}|E(z,t)|$, specially, the color in blue represents the zero fields). It is interesting to note that the transient results versus the observation distance z have different characteristics. The results show irregular variation at observation points closer to the plate $z < 0.8\,\text{m}$ and a similar waveform at observation points away from the plate $z > 0.8\,\text{m}$, whose envelop decreases with the increase of the observation distance. The frequency-domain results obtained by nfTDPO-FFT and nfFDPO are compared in Fig. 3(b). The results show an excellent agreement (less than 0.015 dB) over the range of observation distances 0.05 m to 2.0 m and frequency range of 8 to 12 GHz. Since the frequency-domain data are assumed band-limited, the time-domain result is, strictly speaking, of infinite extent. Noting that the incident waveform and the transient results have been truncated in time, aliasing noise can be expected at two edges of the frequency band when performing the Fourier transform to the nfTDPO results. Thus, the accuracy of nfTDPO is little worse at the two edges of X band (see Fig. 3(b)). The average path number of nfTDPO, nfFDPO and TD-GLQ4 is also given in Table 1, and the ratio of the computation time of nfTDPO and TD-GLQ4 method is about 1 : 528 in this example.

Finally, the near-field scattering from a complex object, a missile model (see Fig. 4(a)), is analyzed. The missile is illuminated by a plane wave whose propagation direction $\hat{\mathbf{k}}_i = -\hat{\mathbf{x}}$, and whose electric field vector has only y component. The PO lit region is shown in Fig. 4(b). The transient electric field versus the light distance ct obtained by nfTDPO is plotted in Fig. 5(a). Considering the distance from the observation point to the different parts of the lit region, it is found that the earlier response in Fig. 5(a) is the transient scattering from the head of the missile (Part A in Fig. 4(b)), and the later response is the transient scattering from the tail of this missile (Part B in Fig. 4(b)). It is worth noting that there is no significant scattering from the remaining surfaces of this missile (such as the horizontal wings etc., Part C in Fig. 4(b)). It is because these surfaces are substantially parallel to the incident direction, and

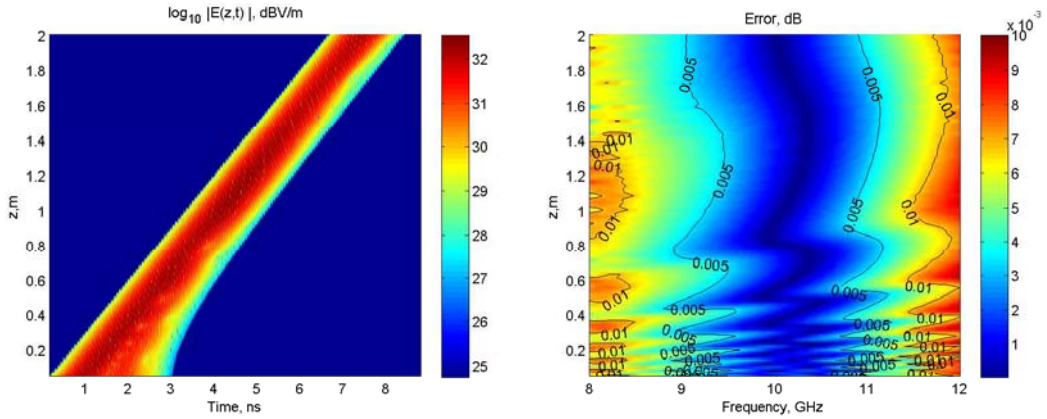

(a) (b)

Figure 3. (a) The near-field electric-field versus time and the observation distance. This result is obtained by nfTDPO for the observation distance z varying from 0.05 m to 2.00 m. (b) The error of frequency-domain results obtained by nfTDPO-FFT and nfFDPO. The result shows an excellent agreement over the range of observation distances 0.05 m to 2.0 m and frequency range of 8 to 12 GHz.

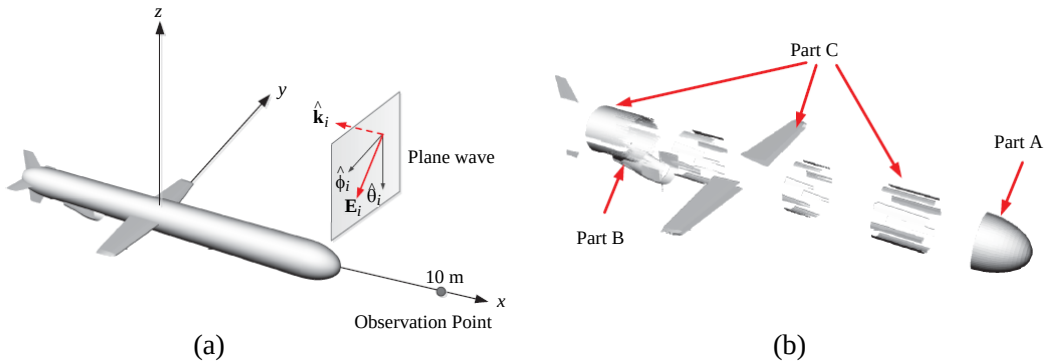

Figure 4. ((a) Near-field transient scattering from scattering from a missile at $x = 10\,\text{m}$, $y = z = 0\,\text{m}$ (refers to Fig. 1). (b) PO lit region.

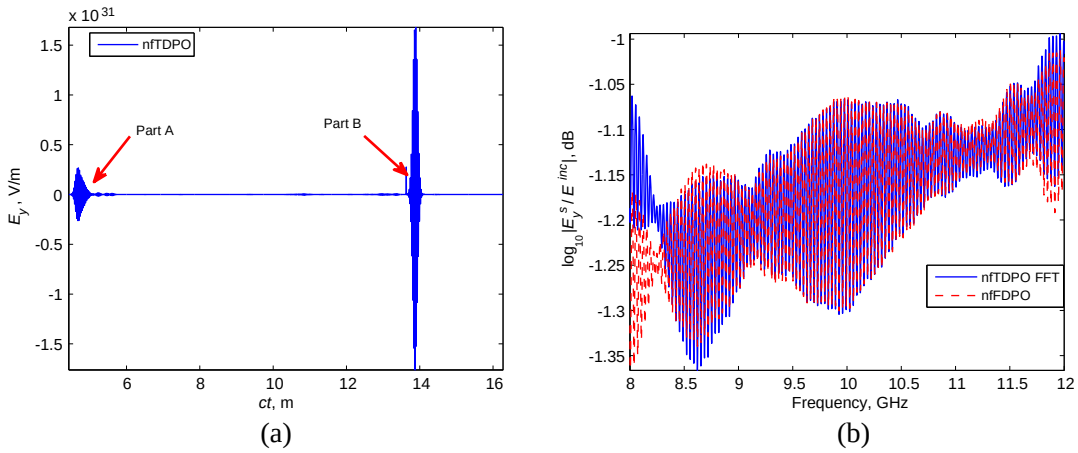

Figure 5. (a) The transient response of backscattering from a missile at $x = 10\,\text{m}$, $y = z = 0\,\text{m}$ (refers to Fig. 1). (b) The normalized wideband frequency-domain results of backscattering from the missile.

the observation point is very close to their tangent plane. There is also no significant scattering from the whole body of this missile for x or z polarization (maximum value is about $10^{27}\,\text{V/m}$) compared with y-polarized result (maximum value is about $10^{31}\,\text{V/m}$. see Fig. 5(a)). It is because these results are obtained by physical optics without considering the contribution diffracted from the edges of the surface (such as physical diffraction theorem). The wideband FD result obtained by nfTDPO-FFT is also compared to the nfFDPO result. As can be seen, the aliasing noise becomes significant for the scattering problem of complex targets. The computation times of nfTDPO, nfFDPO and TD-GLQ4 method are then given in Table 1. As we can see, the speed of the computation time of nfTDPO is better than nfFDPO in this example because more sampled frequencies (4001) are needed for these high oscillation results.

4. CONCLUSIONS

In this paper, a time-efficient method to calculate the near-field time-domain physical-optics integral is developed for analysis of transient fields scattering from 3D PEC targets illuminated by a pulsed plane wave. We reduce the TD-PO surface integral to a close-form representation by introducing locally expanded time-domain Green function approximations. Only functional evaluations are required in these closed-form expressions without quadrature errors, and the evaluation performs more efficiently than numerical quadrature techniques. However, since the number of spatial sampling points for the proposed formulas is sensitive to the distance between the observation points and the PO lit region, the

evaluation of these closed-form expressions has no advantage compared with the numerical quadrature techniques, when the observation points are very close to the targets. To satisfy causality (the transient field cannot travel away from the sources faster than the speed of light), we give the time-domain condition of excitation wave. Numerical examples that prove the accuracy of the proposed closed-form expressions and that demonstrate the efficacy of employing these formulas have been presented. In future work, we will apply the present formula to the time-domain shooting and bouncing ray methods to analyze more complicated near-field transient scattering problem.

REFERENCES

1. Sun, E.-Y. and W. Rusch, "Time-domain physical-optics," *IEEE Transactions on Antennas and Propagation*, Vol. 42, No. 1, 9–15, 1994.
2. Sun, E.-Y. and W. V. T. Rusch, "Time-domain physical-optics analysis of large reflector antennas," *Antennas and Propagation Society International Symposium, AP-S, Merging Technologies for the 90's, Digest*, Vol. 1, 26–29, 1990.
3. Guan, Y., S.-X. Gong, S. Zhang, B. Lu, and T. Hong, "A novel time-domain physical optics for computation of electromagnetic scattering of homogeneous dielectric objects," *Progress In Electromagnetics Research M*, Vol. 14, 123–134, 2010.
4. Le Bolzer, F., R. Gillard, J. Citerne, V. Fouad Hanna, and M. Wong, "A time-domain hybrid method combining the finite-difference and physical-optics methods," *Microwave and Optical Technology Letters*, Vol. 21, No. 2, 82–88, 1999.
5. Qin, S.-T., S.-X. Gong, R. Wang, and L.-X. Guo, "A TDIE/TDPO hybrid method for the analysis of TM transient scattering from two-dimensional combinative conducting cylinders," *Progress In Electromagnetics Research*, Vol. 102, 181–195, 2010.
6. Zhou, X. and T. J. Cui, "A closed-form representation of time-domain far fields based on physical optics," *IEEE Antennas and Wireless Propagation Letters*, Vol. 11, 965–968, 2012.
7. Gordon, W. B., "Far-field approximations to the Kirchoff-Helmholtz representations of scattered fields," *IEEE Transactions on Antennas and Propagation*, Vol. 23, No. 4, 590–592, 1975.
8. Bölükbaş, D. and A. A. Ergin, "A radon transform interpretation of the physical optics integral," *Microwave and Optical Technology Letters*, Vol. 44, No. 3, 284–288, 2005.
9. Legault, S., "Refining physical optics for near-field computations," *Electronics Letters*, Vol. 40, No. 1, 71–72, 2004.
10. Hansen, T. and A. D. Yaghjian, *Plane-wave Theory of Time-domain Fields,* IEEE Press, 1999.
11. Martínez-Búrdalo, M., L. Nonidez, A. Martin, and R. Villar, "Near-field time-domain physical-optics and FDTD method for safety assessment near a base-station antenna," *Microwave and Optical Technology Letters*, Vol. 39, No. 5, 393–395, 2003.